J Infrared Milli Terahz Waves (2010) 31:143–150
DOI 10.1007/s10762-009-9579-2

Development of the Measurement System of Image Rejection Ratio for the Sideband-Separating Receiver

Taku Nakajima · Takeshi Sakai · Nario Kuno · Hideo Ogawa

Received: 16 June 2009 / Accepted: 11 September 2009 /
Published online: 24 September 2009
© Springer Science + Business Media, LLC 2009

Abstract We developed a measurement system of image rejection ratio for the sideband-separating receiver. This system comprises a horn moved by a motor slider, a harmonic mixer and a signal generator. We have installed the system on the Nobeyama 45-m millimeter telescope and compared the image rejection ratio measured by this system with that obtained from molecular line observations of celestial objects. We confirmed that we can measure image rejection ratio with an accuracy of ±10% with our system. By using the system, we can tune the applied bias voltage of mixer chips to the best performance of image rejection ratio and accurate calibration of the intensity of molecular line observations becomes possible. This is the first IRR measurement system developed for practical use with the 2SB receiver system.

Keywords Millimeter wave length · SIS mixer · Sideband-separating (2SB) mixer · Image rejection ratio

1 Introduction

The sideband-separating (2SB) mixer is a superconductor-insulator-superconductor (SIS) mixer and has the ability to observe signals in both the upper (USB) and lower sidebands (LSB) independently and simultaneously by waveguide circuit [1]. It has some advantages over other techniques in operating the mixer receivers in the single sideband (SSB) mode

T. Nakajima (✉) · N. Kuno
Nobeyama Radio Observatory, National Astronomical Observatory of Japan, 462-2 Nobeyama, Minamimaki, Minamisaku, Nagano 384-1305, Japan
e-mail: nakajima@nro.nao.ac.jp

T. Sakai
Institute of Astronomy, The University of Tokyo,
2-21-1 Osawa, Mitaka, Tokyo 181-0015, Japan

H. Ogawa
Department of Physical Science, Graduate School of Science, Osaka Prefecture University,
1-1 Gakuen-cho, Naka-ku, Sakai, Osaka 599-8531, Japan

for spectral-line observations in millimeter and sub-millimeter wave band. First, the waveguide-type 2SB mixer is free from the quasi-optical SSB filter (e.g. Martin-Puplett interferometer) for the separation of sidebands. The loss with the quasi-optics results in a degradation of the system noise temperature. Since the 2SB mixer is composed of waveguide circuits, the loss with the quasi-optics is reduced. Secondly, the 2SB mixer has no tuning mechanics (e.g. backshort tuners) and the gain of the receiver is stable. Recently, a waveguide-type 2SB mixer receiver system is being developed for the Atacama Large Millimeter/sub-millimeter Array (ALMA) (e.g. [2–4]). To date, the simultaneous detection of molecular emission lines with a waveguide-type 2SB receiver has been performed by a few groups toward a limited number of observations [5, 6], suggesting that the 2SB receiver systems are more efficient compared to the other SSB receivers [7, 8].

For the 2SB mixer, the image rejection ratio (IRR), which is the value of rejecting power from the image sideband to the signal sideband in the heterodyne mixer receiver in SSB mode, depends on the quality of SIS chips and is changed by tuning the SIS bias voltage. Therefore, we have to check the IRR before each observation. We have developed a new measurement system for the IRR and installed this system on the 2SB receiver in the 45-m millimeter wave telescope at Nobeyama Radio Observatory (NRO)[1] in Nagano, Japan. Using this measurement system, the applied bias voltage of the SIS chips can be tuned to the best performance of the IRR and we can improve the accuracy of the absolute intensity of molecular line. This is the first IRR measurement system developed for practical use.

In the present paper, we describe the IRR measurement system for the 2SB receiver in the 100-GHz band. The results of comparison between the value of IRR measured by the measurement system and that obtained from molecular line observations of celestial objects are also presented.

2 Device configuration

A block diagram of the receiver system and the measurement system of the IRR is shown in Fig. 1. The IRRs were evaluated by measuring the relative amplitudes of the IF responses in the USB and LSB injecting a continuous wave (CW) signal generated by multiplying the output of the signal generator (SG) with the harmonic mixer to observation frequency band. The test signal generated by the SG is from about 8 to 11.5 GHz and is multiplied by a factor of ten. The signal is injected into the 2SB mixer by a horn. The horn is moved (in parallel) by a motor slider made by the ORIENTAL MOTOR Co. Ltd. on top of the receiver dewar. It is located out of the beam from the main reflector during observations of celestial objects (Fig. 2a) and inserted in the beam center only at the measurement of the IRR (Fig. 2b). Not the feed horn but the amputated waveguide is used to prevent a standing wave between the horn of the measurement system and receiver horn. Thus, the aperture of the horn is the rectangular shape of the W-band. Moreover, an isolator is also used to prevent the standing wave between the horn of the measurement system and the harmonic mixer. When the IRRs are measured, the IF signals from the 2SB mixer are input to the spectrum analyzer. The USB and LSB signals are selected by coaxial switch. We use the LabVIEW program [9] for acquisition of data, control of equipment, and calculation of the IRR

[1] The Nobeyama Radio Observatory is a branch of the National Astronomical Observatory of Japan, National Institutes of Natural Sciences; http://www.nro.nao.ac.jp/index-e.html.

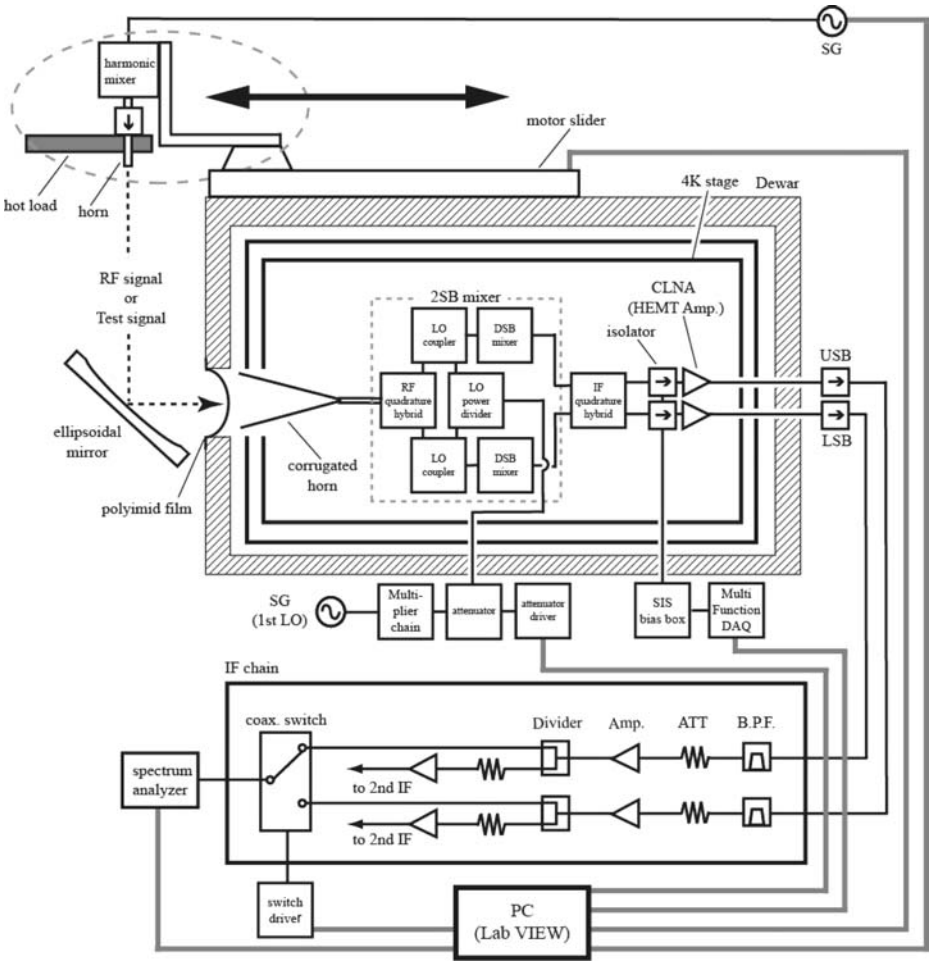

Fig. 1 Block diagram of the 2SB receiver system. The figure shows the IRR measurement system, receiver dewar, and IF chain from above.

3 Calculation and measurement of IRR

We adopted the Kerr *et al.* [10] method to calculate the IRRs, R_1 and R_2 with the following formulae:

$$R_1 = M_U \frac{M_L M_{DSB} - 1}{M_U - M_{DSB}} \tag{1}$$

and

$$R_2 = M_L \frac{M_U - M_{DSB}}{M_L M_{DSB} - 1} \tag{2}$$

where M_U is the ratio of powers with a CW test signal in the USB, the corresponding IF signals at USB (signal band) and LSB (image band) IF ports (Fig. 3a). M_L is the ratio of powers with a

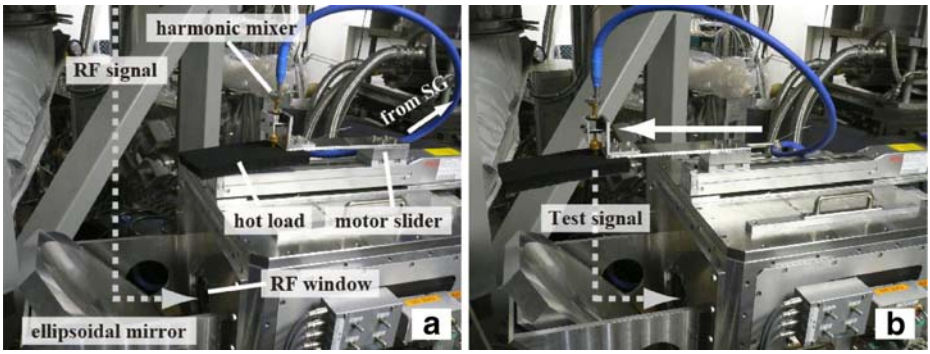

Fig. 2 Photograph of the IRR measurement system on the top of the receiver dewar. It is located out of the beam from the main reflector during observations (**a**) and inserted in the beam center only at the measurement of IRR (**b**).

CW test signal in the LSB, the corresponding IF signals at LSB (signal band) and USB (image band) IF ports (Fig. 3b). M_{DSB} is the ratio of the difference of output power at USB (ΔP_1; Fig. 3c) and LSB (ΔP_2; Fig. 3d) when injecting the radiation of the hot and cold loads. That is, this method requires two variant temperatures, hot and cold loads. We use the radiation from the absorber of ambient temperature for hot load and the radiation of the sky for cold load. But the radiation of the sky has to remain stable through the measurement. The measured quantities M_U , M_L , and M_{DSB} can now be used to deduce $R_1$and R_2 .

The measuring procedure is as follows. The measurements are all automatic operations by the software of the LabVIEW.

1. The IF power of the USB and LSB are measured when the sky radiation as cold load is input to the 2SB receiver.
2. The radiation of hot load is input to the receiver and the IF powers are measured.
3. The ΔP_1 and ΔP_2 are calculated from 1 and 2. Then M_{DSB} is calculated from ΔP_1 and ΔP_2.
4. The horn of the measurement system is moved to the center of the beam from the main reflector.
5. The USB test signal is input to the receiver and the IF power of the USB (signal band) is measured.
6. The coaxial switch is changed and the IF power of the LSB (image band) is measured.
7. The M_U is calculated from 5 and 6.
8. The LSB test signal is input to the receiver and the IF power of the LSB (signal band) is measured (Fig. 3d).
9. The coaxial switch is changed and the IF power of the USB (image band) is measured (Fig. 3c)
10. The M_L is calculated from 8 and 9.
11. The R_1 and R_2 are calculated from 3, 7 and 10.

We can measure the IRR between 5 and 7 GHz of IF with a frequency step chosen by the observer. For example, it takes about 3 min for the measurement at 11 points, that is, a 200 MHz interval.

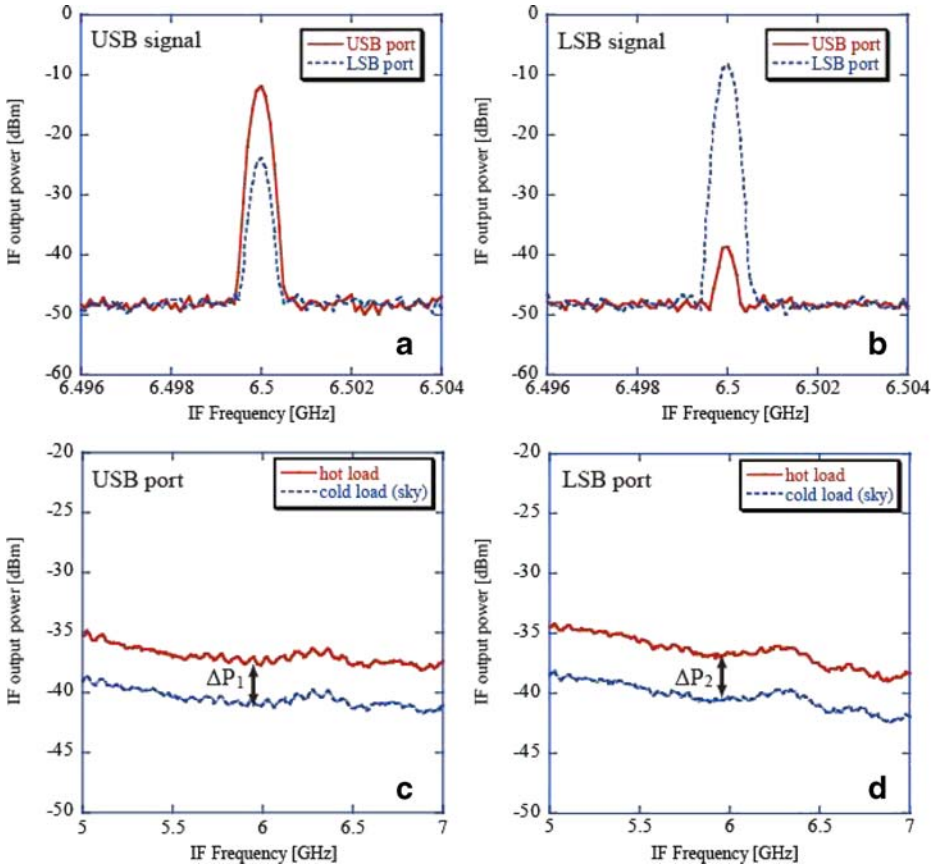

Fig. 3 The IF power in the hot (bold line) and cold load (dashed line) of the USB (**a**) and LSB (**b**) shown as functions of the IF frequency. The difference in output power at USB is ΔP_1 and LSB is ΔP_2 when injecting the radiation of hot and cold loads. The IF power output of USB port (**c**) and LSB port (**d**) when injecting the test signal of USB (bold line) and LSB signal (dashed line).

4 Tuning of 2SB SIS mixer

First of all, we decided the tuning parameters of the receiver when changing the bias voltage for two SIS chips in the 2SB mixer and power of the local (LO) signal. The parameter measurement is performed in the LO frequency range of 80 to 116 GHz with an interval of 2 GHz. The IRR and the SSB noise temperature of the system, including the atmosphere (T_{sys}), are measured at the same time. We adopted the combination of the SIS bias voltage and LO power which achieves the minimum value of T_{sys} and more than 10 dB of IRR as a parameter. Figure 4 shows the example of the result of a measurement of the IRR and T_{sys}. The tendency is different because of the USB and the LSB and the IRRs are inversely correlated. The point where T_{sys} is minimum does not become maximum IRR. This tendency hardly depends on the power of LO. The bias voltage of two SIS chips in the 2SB mixer and the power of LO signal input to the 2SB mixer are automatically set at the observation. We prepare the parameter table of three patterns, observation of only USB, only LSB and simultaneous observation of USB and LSB.

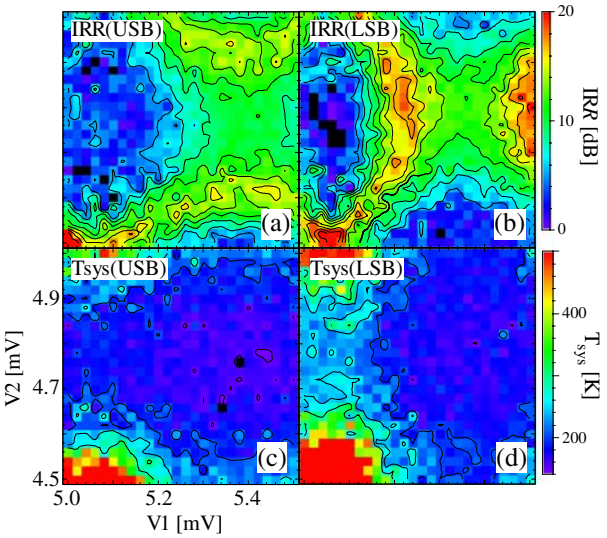

Fig. 4 The IRR and T_{sys} of USB (**a**), (**c**) and LSB (**b**), (**d**) to combination of two SIS bias voltages.

5 Results

Figure 5 shows the relation between the IRR value measured by the IRR measurement system and that estimated from the molecular line observation toward the W51 molecular cloud. We get the integrated intensity and measured the IRR when the SIS bias voltages for the 2SB mixer were changed by seven points. Each measurement was done continuously five times. The standard deviation is shown as an error bar of the IRR. The integrated intensity of the signal is measured by the observations of ^{13}CO (J=1–0) in USB and that of

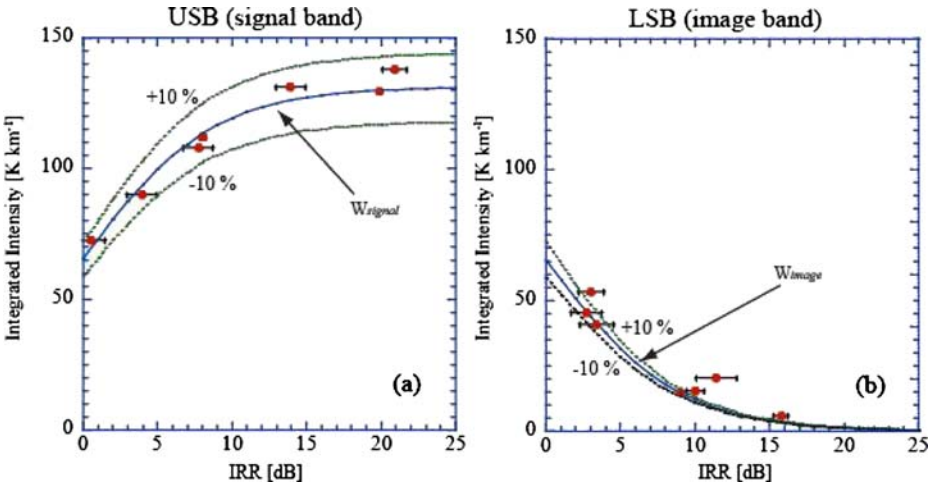

Fig. 5 The relation between the IRR value measured by the IRR measurement system and the integrated intensity estimated from the molecular line observation in USB (**a**) and LSB (**b**), respectively. The bold line shows the anticipated value of the IRR according to the IRR calculation formula, and the dashed lines represent an error range of ±10%.

the image is measured in LSB. The error margin calculated from the rms noise level was shown as the vertical error bar. The bold line shows expected value of IRR according to the following IRR calculation formulae and the dashed lines show an error range of ±10%. The integrated intensity of the signal band (W_{signal}) and image band (W_{image}) are

$$W_{signal} = \frac{W_{real}}{1 + \frac{1}{R_1}} \tag{3}$$

and

$$W_{image} = \frac{W_{real}}{1 + R_2}, \tag{4}$$

respectively. It is assumed that optical depth of signal band (τ_{USB}) and image band (τ_{LSB}) are equal. Where W_{real} is the standard integrated intensity of independent observation estimated by another receiver on the NRO 45-m telescope toward W51 with ^{13}CO (J=1–0), which is 131 K km^{-1}. The value of the IRR measured by the measurement system and that measured by the observations ranges from −3.9 to +6.1% for the signal band (Fig. 5a) and from −1.3 to +134.2% for the image band (Fig. 5b). At least the signal band is consistent within an accuracy of ±10%. The error of IRR is mainly due to the reading accuracy of signal intensity by the spectrum analyzer. The large deviation from calculation value is thought to be due to a pointing error caused by the wind.

6 Conclusions

We have developed an IRR measurement system and installed the system on the 2SB receiver in the NRO 45-m millimeter telescope. The IRR value measured by this system and that measured by the observations are consistent within an accuracy of ±10%. Therefore, we can obtain the best tuning of the 2SB mixer with the system to improve the accuracy of intensity calibration of molecular line observations. This is the first IRR measurement system developed for practical use with the 2SB receiver system.

Acknowledgement The authors would like to thank the entire staff of the Nobeyama Radio Observatory for their useful discussions and support. This study was supported in part by a Grant-in-Aid for Scientific Research on Priority Areas (15071205) from MEXT.

References

1. S. M. X. Claude, C. T. Cunningham, A. R. Kerr, and S.-K. Pan, “Design of a Sideband-Separating Balanced SIS Mixer Based on Waveguide Hybrids,” ALMA Memo 316 (2000).
2. C. C. Chin, D. Derdall, J. Sebesta, F. Jiang, P. Dindo, G. Rodrigues *et al*., “A Low Noise 100 GHz Sideband-Separating Receiver,” Int. J. Infrared Millim. Waves **25** (4), 569–600 (2004).
3. A. R. Kerr, S.-K. Pan, E. F. Lauria, A. W. Lichtenberger, J. Zhang, M. W. Pospieszalski *et al*., “The ALMA Band 6 (211–275 GHz) Sideband-Separating SIS Mixer-Preamplifier,” ALMA Memo 498 (2004).
4. M. Kamikura, Y. Tomimura, Y. Sekimoto, S. Asayama, W. Shan, N. Satou *et al*., “A 385–500 GHz Sideband-Separating (2SB) SIS Mixer Based on a Waveguide Split-Block Coupler,” Int. J. Infrared Millim. Waves **27** (1), 37–53 (2006).

5. S. Asayama, K. Kimura, H. Iwashita, N. Sato, T. Takahashi, M. Saito *et al*., "Preliminary Tests of Waveguide Type Sideband-Separating SIS Mixer for Astronomical Observation," ALMA Memo 481 (2003).
6. E. F. Lauria, A. R. Kerr, G. Reiland, R. F. Freund, A.W. Lichtenberger, L. M. Ziurys *et al*., "First Astronomical Observations with an ALMA Band 6 (211–275 GHz) Sideband-Separating SIS Mixer-Preamp," ALMA Memo 553 (2006).
7. T. Nakajima, M. Kaiden, J. Korogi, K. Kimura, Y. Yonekura, H. Ogawa *et al*., "A New 60-cm Radio Survey Telescope with the Sideband-Separating SIS Receiver for the 200 GHz Band," Publ. Astron. Soc. Jpn. **59**, 1005–1016 (2007).
8. T. Nakajima, T. Sakai, S. Asayama, K. Kimura, M. Kawamura, Y. Yonekura *et al*., "A New 100-GHz Band Front-End System with a Waveguide-Type Dual-Polarization Sideband-Separating SIS Receiver for the NRO 45-m Radio Telescope," Publ. Astron. Soc. Jpn. **60**, 435–443 (2008).
9. National Instruments Corporation, USA, http://www.ni.com/.
10. A. R. Kerr, S.-K. Pan, and J. E. Effland, "Sideband Calibration of Millimeter-Wave Receivers," ALMA Memo 357 (2001).